Revue des Composites et des Matériaux Avancés-Journal of Composite and Advanced Materials
Vol. 34, No. 4, August, 2024, pp. 533-540
Journal homepage: http://iieta.org/journals/rcma

Z-scan Study of the Non-linear Optical Properties of Silver/Curcumin Dye Nanocomposites Prepared Via Nanosecond Pulsed Laser Ablation

Nadia Mohammed Jassim[1*], Nada Ismael Ibrahim[1], Nasreen Zaidan Khalaf[2]

[1] College of Science, Diyala University, Diyala 4200, Iraq
[2] Ministry of Education, Directorate General for Education, Diyala 4200, Iraq

Corresponding Author Email: nadiajassim@uodiyala.edu.iq

https://doi.org/10.18280/rcma.340415

Received: 22 April 2024
Revised: 29 May 2024
Accepted: 25 June 2024
Available online: 27 August 2024

Keywords:
non-linear and linearoptics, silver nanoparticles, plasmonics, X-ray diffraction, and curcumin

ABSTRACT

The fabrication related to single-layer Ag/curcumin (Curc) dye nanocomposites on a substrate is described in this paper, along with an examination of optical characteristics that follow, which could be applied to non-linear optics. With the use of a nanosecond pulsed laser method, AgNPs were produced. Using a straightforward solution technique, hybrid Ag/Curc dye nanocomposites have been created with varying concentrations regarding the Curc dye. The impact of concentration on the (non-linear and linear) structural and optical properties was then examined. The following techniques have been examined: FT-IR analysis, FE-SEM microscope, XRD, fluorescence spectroscopy, and UV-Vis spectra. Non linear refractive index as well as non linear absorption coefficients of samples have been utilized in order to explore the non-linear optical (NLO) properties related to the Curc dye nanocomposites and hybrid AgNPs using Z-scan method. A nano-second pulsed Neodymium-YAG laser operating at 532 nm has been employed in the Z-scan approach. The findings demonstrate that the size of AgNPs affects their nonlinearity absorption coefficients and non-linearity refractive index. The enhancement of visual qualities was attributed, according to the data, to an increase in Curc content. For AgNPs and raise the strength of surface plasmon resonance (SPR), which will boost NP production and enhance fluorescence. The absorption which emerges near wave number 3451 cm^{-1} in the infrared Fourier test of AgNPs was researched because it results from the alcohol group's (OH) bond vibration. The aromatic (C-H) bond is the absorption bond 2927 cm^{-1}, indicating that Curc functions as a cover agent. A study was conducted using XRD to examine AgNPs and a hybrid mixture of Curc and AgNPs. XRD data of AgNPs revealed a cubic and polycrystalline crystal structure, with several angles recorded that are exactly the same as the international standard cards for silver. A straightforward platform for improving optical qualities is offered by such hybrid Ag/Curc dye nano composite, which may find use in nano-probing as well as nano-medical applications, including the antibacterial domain.

1. INTRODUCTION

The interaction of light with a high intensity incident laser beam and a material (solid, gas, or liquid) in a non-linear medium is the field of nonlinear optics. Linear optics field is the study of linear behavior of light in a non-strong light field that is not powerful enough to modify the properties of the medium [1-6]. SPR is the term used to describe how much better the metal NPs can support electron excitation in the case when exposed to radiation. The frequency regarding SPR for AgNPs takes place in the visible range of electromagnetic radiation; it could be adjusted by varying the shape and size of the particle and it is based on the real and imaginary parts; as a result, AgNPs cover a broad range of applications in various fields [5, 7-9]. The aim of the work is focused to study and measure the nonlinear optics is considered one of the important to characterize the materials and determine the optical properties of new materials and may be use them in many applications such as modulators [10, 11].

Optical properties for nanomaterials. it is easy technique to measure the nonlinear optical characterize by propagating the laser radiation through the nonlinear crystal materials with the changing the phase $\Delta\Phi$. it is related to the change if refractive index Δn [12, 13].

This work employed the strong and useful Z-scan method to analyze the non-linear optical characteristics regarding a hybrid silver/Curc dye nanocomposite [6, 7]. The formation of a thermal lens around the NPs as a result of the active transport of nanoparticle heat to the center or the difference between refractive index and the matrix represents the true explanation for the Z-scan technique [14-20]. It is considered one of the most commonly useful technologies due to its merits, such as greater sensitivity, ease, and quickness [21, 22]. To make things clearer, the idea of nonlinearity in optics can

be explained as the way light behaves when going past non-linear materials [23]. The intensity parameter on which polarization depends [24].

When a high-power laser beam is incident on the material, the optical material constants such as refractive index and the absorption factor will change. we can derive the equations of nonlinear term from the polarization related to the optical field P(E) [25].

$$P = \varepsilon o[\chi 1\, E + \varepsilon o \chi 2\, E2 + \varepsilon o \chi 3\, E3 + \ldots\ldots\ldots\ldots]$$
$$P = \varepsilon o[\chi 1 E + \chi 2\, \mathrm{EE} + \chi 3\, \mathrm{EEE} + \ldots]$$
$$P = P_L + P_{\mathrm{NL}}$$

The vacuum permittivity is εo and linear susceptibility is termed as χ.

The linear polarization appears in Eq. (1) as the 1st term and other terms in Eq. (1) represent the nonlinear polarization, χ2 and χ3 are the 2nd and 3rd orders of nonlinearity, respectively [26].

González-Castillo et al. [27] created silver nanoparticles by laser and the effect of color solution was studied.

Shanshool et al. [28] in 2016 had studied nonlinear optical properties of polymer nanocomposites of zinc oxide nanoparticles with polymethyl-methacrylate (PMMA) as the polymer matrix.

The present project includes preparing a nano hybrid composite materials, namely silver nanoparticles and curcumin dye, and studying some of the nonlinear properties of these materials prepared by the pulsed laser method ,This project is included some different analysis to above previous studies by highlighting to use more than material to study the nonlinear optical characterization as well as the behavior of the nonlinear characterization depend on the concentration of the materials and the size of nanomaterials.

2. EXPERIMENTAL TECHNIQUES

2.1 Samples preparation

With the use of a high-purity (99.99%) Ag metal as a target and pulsed laser ablation (PLAL) technology in a liquid state are part of the preparation process. Prior to and following each experimental procedure, the Ag metal target has been cleaned with the use of an ultrasonic path device for removing impurities, first washing it with ethanol and after that distilled water. Ag metal target has been immersed in distilled water (DW) as well as placed at the bottom of glass container. Every experimental procedure employed five milliliters of water, and the liquid was raised to a height of four millimeters over the target's surface. The utilized pulsed laser has 530 mJ of energy in each pulse, in which 600 laser pulses at a constant laser energy of 530 megajoules were required to ablate the Ag metal target surface. Additionally, there was a distance of 8 cm between target and laser lens, and laser beam's diameter on Ag metal target's surface was 2 mm. Q-Switched A Nd-Yag pulse laser at 1064 nm was utilized as an ablation system for an Ag metal target with a frequency of 1Hz and a pulse time of 10 nm for obtaining solution which contained a colloidal liquid to change color following the procedure of the ablation.

2.2 Z-scan technique

Nonlinear optical characteristics of Ag/Curc nanocomposites have been examined using the Z-scan method. A simple and very sensitive approach that is used to find n_2 (nonlinearity of the refractive index) as well as n1 (nonlinearity of the absorption coefficient) is the Z-scan method [9, 16-18]. The non-linear characteristics of Ag/Curc dye nanocomposites, which have been created by pulsed laser ablation, are measured using an experimental setup consisting of closed as well as open aperture Z-scan [13, 19, 20]. Figure 1 illustrates it. An Nd-Yag pulsed laser system with fluence intensity of 6.794GW/cm^2 at 532 nm is employed in the experiment. The output laser has been split into two sections using a beam splitter. The transmitted part has been focused by a lens, and this reflected part is the reference (incidental light fluence). The focus has been moved to the sample. Two energy detectors monitored the fluences of the transmitted and incident pulses simultaneously.

A nedymium-Yag Laser Q-switched is using with Z scan technology as a pumping source with a wavelength 1064 nm. Laser radiation is projected in the z-axis on to the target using a lens with a short focal length. A target makes a move throughout the length of the z-direction, going past the focal point of the lens at z = 0 [27, 29-31].

The transmittance intensity of laser beam was measured at z-direction by a closed aperture with the position change of the target (z). In the state of the open aperture of the Z-scan, the transmittance intensity is collected by a lens through the target. The experimental system has been drawn in Figure 1. Samples were moved across the lens's focal plane with an 8.5 mm focal length and polarizer along optical axis (Z-direction).

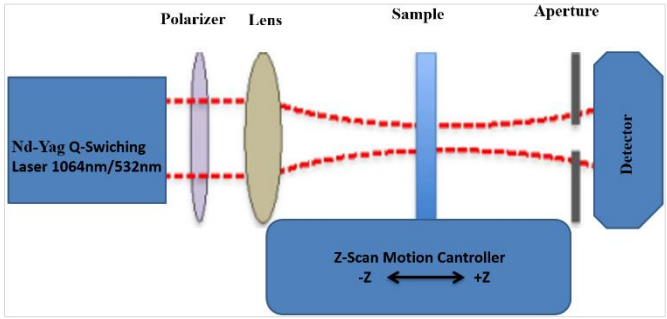

Figure 1. Z-scan experimental setup

The Z-scan method measures refractive index variation related to incident laser intensity and is dependent on the refractive index-related intensity. For every sample position, the induced lens inner the target has a variable focal length, which is determined by the laser beam's intensity. The laser beam has been concentrated, and the target has been scanned through a Gaussian beam (TEM00) via its focal plane in order to evaluate the nonlinearity response. By using of a finite aperture at far field, laser beam intensity for every point as a function of focus position has been measured. Also, input beam has been split through a beam splitter and detected by an appropriate system of detection in order to determine the laser's total beam intensity. Non-linear refraction coefficient's sign and value may be measured thanks to the closed aperture. In the case when the non-linear refractive index of the medium is negative, a typical peak-to-valley transmittance curve is acquired because the light intensity that is irradiated on the sample varies at every position. When a sample has a negative refraction index, it acts like a concave lens close to the focus point. The focused position shifts to the positive Z direction as the sample approaches the focal point and the negative Z position. As a result, the intensity at the detector increases, and

the beam at the aperture plane is suppressed. The beam widens at aperture, and intensity rises on the positive side as the sample approaches the focal point and the positive position of Z.

3. RESULTS AND DISCUSSION

Ag/Curc dye nanocomposites' non-linear optical properties control the localized SPR effect. Figure 2 displays UV-Vis absorption spectra of Curc dye, AgNPs, and Ag/Curc dye nanocomposites (measured with a Perkin Elmer instrument).

The impact of elevating the Curc dye concentration on the optical characteristics of AgNPs was examined within the range of 100-1200 nm in wavelength. The absorption spectrum reveals that the production Ag/Cur dye nanocomposite reaches its maximal absorption spectrum at 420 nm. The localized SPR of pure AgNPs is 418 nm, and the localized SPR of pure Curc dye is 312 nm. Peak absorption varied between samples for AgNPs, Curc dye, and Ag/Curc dye nanocomposites, which was attributed to absorption of diverse particle sizes and diameters. Free electron oscillations in conduction band, occupying the energy levels near Fermi level, are what give metal NPs their plasmon surfaces [11].

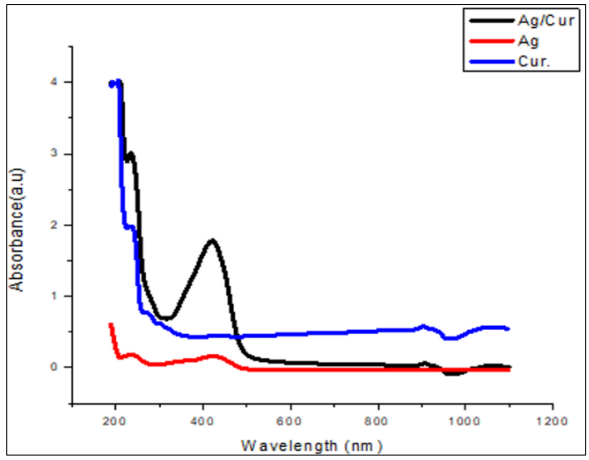

Figure 2. UV-visiblespecroscopy of Curc dye, AgNPs and Ag/Curc dye nanocomposites

Figure 3. showed the morphological properties of samples by taking FE-SEM images of Figure 3(a) and (b) low and high significance images of silver nanoparticles, (c) and (d) low and high significance images of silver/Curc nanocomposites.

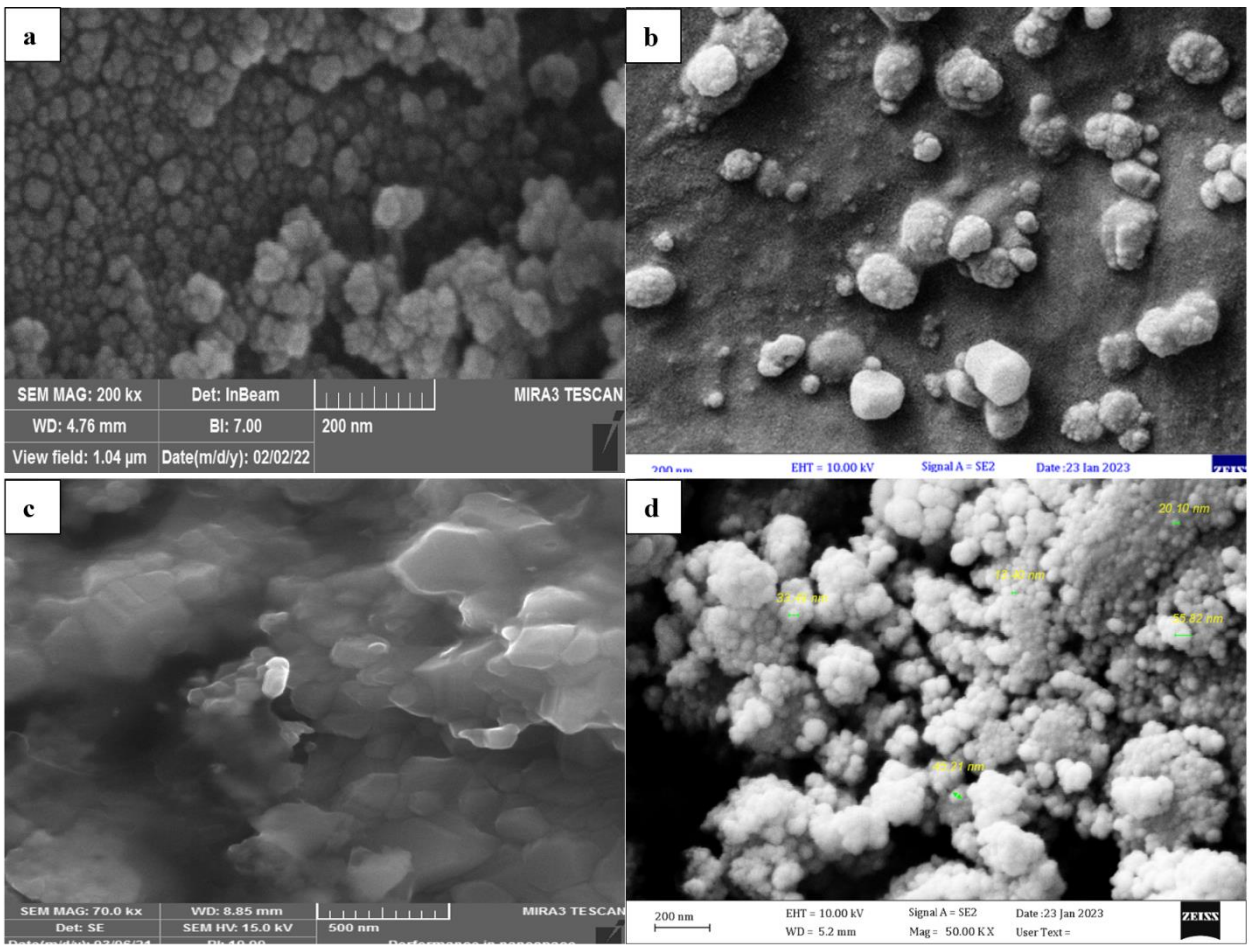

Figure 3. FE-SEM images: (a) Low significance images of silver nanoparticles; (b) High significance images of silver nanoparticles; (c) Low significance images of silver/Curc nanocomposites; (d) High significance images of silver/Curc nanocomposites

The isotropic shape regarding the AgNPs allowed for the suitable calculation of the related LSPR peaks based on the obtained absorption result. EDX is employed in this examination to identify the components of samples and exhibits the presence of chemical elements depending on their atomic and weight ratios. The sample (AgNPS) prepared to (600) pulses as well as ablation energy 600mJ in a distilled water medium which contain (O, Ag, Au, C) elements, a few

of them are elements that are present in surrounding atmosphere (EDX) device, is shown in Figure 4. Upon coating inner surface of the device (EDX) with gold metal, we observe the appearance related to the highest peak of gold (Au), as shown in Table 1.

Table 1. Exhibits percentages of the elements (AgNps)

	Elements	wt.%	at.%
Ag47	K-series	62.63	18.45
O8	K-series	26.29	52.23
C6	K-series	11.08	29.32
	Total	100.00	100.00

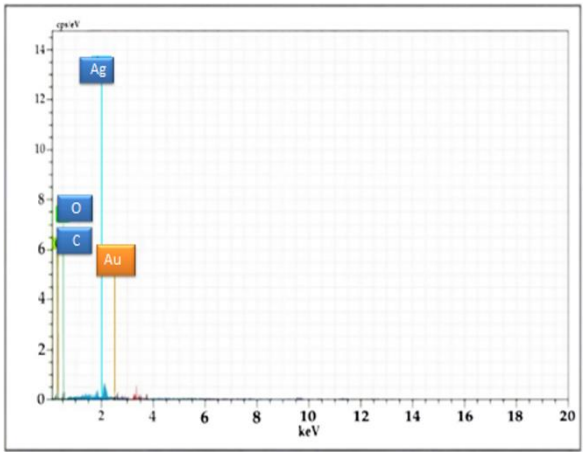

Figure 4. EDX of the sample (AgNps)

EDX diagram of the sample (AgNPS) formed in distilled water medium including elements (O, Ag, Si, C, Au) with (600) pulses and 600mJ ablation energy is shown in Figure 5. The device (EDX) has been coated with gold metal on its inner surface, causing the highest peak of gold (Au) to show. Some of these elements are found in the surrounding atmosphere, as Table 2 shown.

Table 2. Exhibits percentages of the elements (AgNps)

	Elements	wt.%	at.%
Ag47	K-series	52.3	48.18
Si14	K-series	18.8	6.91
O8	K-series	16.8	6.42
C6	K-series	12.1	38.49
	Total	100.00	100.00

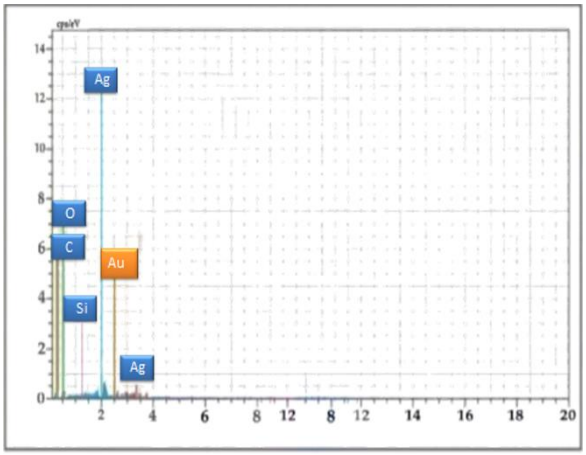

Figure 5. EDX of the sample (AgNps-Cum)

Determining Fourier transforms via infrared spectroscopy is a crucial method for the examining of bonds among atomic components in Ag solutions, since it includes AgNPs functional groups. The link between wave number and transmittance in the 500-4,000 IR spectrum regarding Ag NPs produced in distilled water (D.W.) with pulse numbers (600) and a constant ablation energy (530mJ) is shown in Figure 6. It is evident that (Ag-O) bond is responsible for absorption bond near wave number (667.27 cm^{-1}), stretching (C-O) group, a vinyl ether group, is responsible for absorption bond near wave number (1045.42 cm^{-1}), and stretching (C-O) group is responsible for absorption bond close to number (1634.30 cm^{-1}).

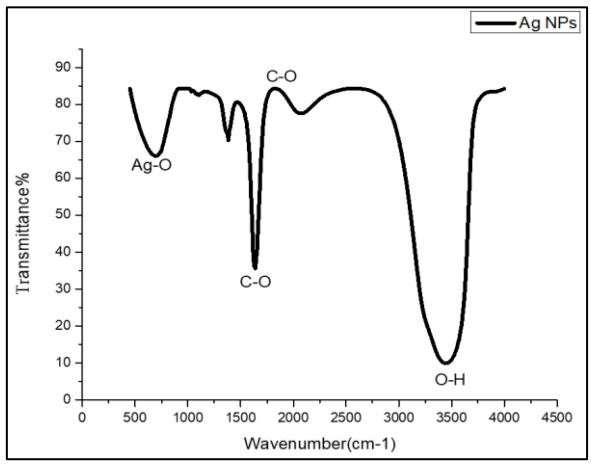

Figure 6. FTIR spectrum of a solution of AgNPs

According to Figure 7, aliphatic (OCH_3(C-H)) group is responsible for absorption bond near wave number 2997 cm^{-1}, while absorption bond near wave number (3,451) is the result of (OH) bond vibrating back to the alcohol group. Aromatic (C-H) bond is the absorption bond 2927 cm^{-1}, while (C-O) group is responsible for the bond for the wave number 1085 cm^{-1}. Near wave numbers (1651 and 1645 cm^{-1}, respectively), the absorption bonds are aromatic (C = C) and aliphatic (C = C). This illustrates the capping agent role of Curc.

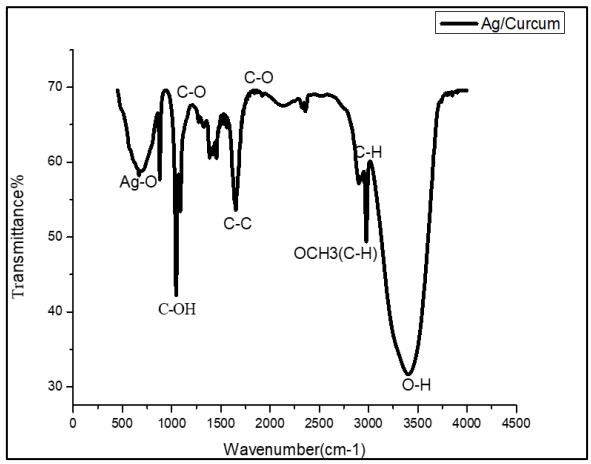

Figure 7. FTIR spectrum of a solution of (AgNps-CUM)

The nonlinear refractive index (n_2) could be found by applying the Z-scan approach, which measures nonlinear absorption as well as nonlinear refraction simultaneously in a variety of media, including liquids, solids, and liquid solutions. The refractive index sign and magnitude of the non-linearities

are obtained using a single-beam technique. With the use of Z-scan method, useable data was obtained by moving the sample backward or forward along the path of femto-second laser beam and through its focal point. Non-linear optical effects were seen in the area around the focus point, in which the laser intensity has been quite high. Z-scans with closed and open apertures have been employed to distinguish between NLR and NLA effects for every layer of nanoparticles. A negative non-linear refractive index, commonly referred to as self-defocusing, was proposed through the pattern of a peak followed through a valley in normalized transmittance data for closed-aperture Z-scan test. The aperture linear transmission in such case has been 0.245.

We used both closed-as well as open-aperture Z-scan methods to analyze Ag/Curc dye nanocomposite films for calculating the non-linear coefficients (Table 3). Ag/Curc dye nanocomposite film far field open-aperture transmission was investigated to determine all non-linear absorption coefficients.

Table 3. The changing transmittance results for closed aperture Z-scan

Samples	Particle Size	Tmax	Tmin.	ΔTpv	n_2 cm²/GW
S_1	17.93	1.1	0.8	0.3	-0.2312
S_2	26.89	0.9	0.5	0.4	-0.215
S_3	29.31	1.6	1.1	0.5	-0.204

Non-linear absorption in Ag/Curc dye nanocomposite films is specified by Figure 8, which displays decreases in transmittance around focal point of scanned samples at various thicknesses [1]. S_1 and S_2's increment trend was not the same as S_3's. The shift of S_3 on peak and strong T (peak to valley distance) indicate that all of the films exhibit reverse saturable absorption [12]. Open-aperture graphs displayed peaks and valleys throughout. We concentrate on the non-linear refractive index (n_2) of Ag/Curc dye nanocomposite films in order to assess the refractive non-linearity. Closed-aperture measurements have been made for this, and the normalized transmittance is displayed in Figure 8. The post focal peak and valley seen in Ag/Curc dye nanocomposite films is a specific indicator of positive n_2 (positive lens).

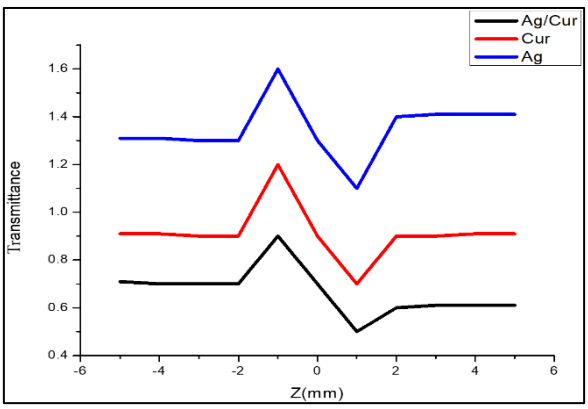

Figure 8. Closed aperture Z-scan curve for samples (a) Curc dye; (b) silver nanoparticles; (c) Silver/Curc nanocomposites

Figure 8 shows negative z-scan patterns for both samples, indicating a self-defocusing effect. When there is a negative Z-scan profile that begins far from focus (Z<0), there is little non-linear refraction and minimal beam flounce; as a result, the measured transmittance is z-independent and stays constant. The next equation could be used to get the nonlinear refractive index, or n_2, in a closed aperture Z-scan [11].

$$n_2 = \Delta\varphi_0 / I_0 \, L_{\text{eff}} K \tag{1}$$

where, K = 2π/λ, $\Delta\varphi_0$ = non-linear phase shift, I_0 represents intensity at the at the focal point and Leff: represents effective length of the sample that can be calculated from the Eq. (2) [11]:

$$\text{Leff} = (1 - e^{-\alpha 0 L})/\alpha 0 \tag{2}$$

where,

$\alpha 0$: represents linear absorption coefficient

L: represents sample length

Intensity at focal spot can be expressed as Eq. (3) [12]:

$$Io = 2Ppeak/\pi\omega 0 \tag{3}$$

where,

$\omega 0$: represents beam radius at focal point

Ppeak: the peak power given by the Eq. (4) [12]

$$Ppeak = E/\Delta t \tag{4}$$

where, S_1: Ag NPs; S_2: Curcumin dye and S_3: Ag/Curcumin nanoparticles

The primary explanation for this could be the measured and characteristic size of NPs. According to the current study, the size of the Ag NPs, which is 17.93 nm, is smaller than that of the Curc dye, which is 26.89 nm, and it is also significantly smaller compared to the Ag/Curc nanocomposites, which have a particle size of 29.31 nm. Since the cubic non-linearity is predicted to scale with particle volume, the size of NPs will directly impact the intensity of the transmitted laser. The outcomes above show a strong correlation [13, 18-20].

Non-linear absorption coefficient (β) was study by open aperture Z-scan by collecting transmitted laser light, and can directly measure from the transmittance curves and it's given by the Eq. (5) [11].

$$T(z) = \sum_{m=1}^{\infty} \left(\frac{\beta I \, \text{Leff}}{1 + \left(\frac{Z}{Z0}\right)^2} \right)^m \frac{}{(m+1)3/2} \tag{5}$$

where,

Z: represent sample's position with minimal transmittance

Zo: represent diffraction length

m: number integer

T(z): represent minimal transmittance

The two terms in the sum are in general sufficient for determining the value of β, which is the non-linear absorption coefficient.

The samples (Curc dye, Ag NPs, and Ag/Curc nanocomposites) exhibited saturable absorption from the broad SPR band, according to the results of the open aperture Z-scan. It has been discovered to be highly anisotropic, and that could be adequately explained through a straightforward 2-level saturation model.

Figure 9, showed open-aperture Z-scan curve's peak value, ΔT, is displayed. With open-aperture Z-scan, intensity-dependent absorption can be computed more accurately, yet it

is observable with a closed-aperture Z-scan as a change in the transmittance through the sample. The light-matter interaction that takes place in the case when a sufficiently intense laser beam is incident on a sample determines the values of and n_2. The medium's optical characteristics could be altered by such interaction. This work demonstrates that the thickness and size of Ag/Curc dye nanocomposites that were deposited affected the n_2 and n_1 values of the samples; substantially bigger Ag/Curc dye nanocomposites in S_2 had lower and n_2 values compared to those in S_1 nanocomposites. The nonlinear absorption coefficients of silver nanoparticles utilizing the closed-aperture Z-scan with a 532 nm pulsed Nd-Yag laser at three distinct reduction periods was cleared in Table 4.

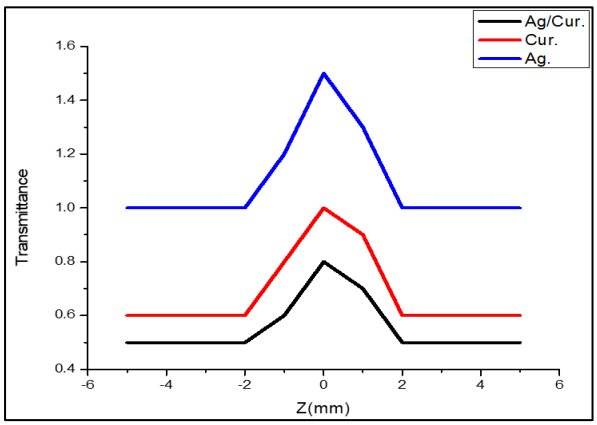

Figure 9. Exhibits open aperture Z-scan curves for samples (a) Curc dye; (b) AgNPs; (c) Ag/Curc nanocomposites

Table 4. The non-linear absorption coefficients regarding Ag NPs utilizing the closed-aperture Z-scan with the pulsed laser Nd: YAG at 532 nm at three distinct reduction periods

Samples	Particle Size	Tmax	β cm/GW
S_1	17.93	1.54	66122.01
S_2	26.89	0.95	3984.52
S_3	29.31	0.78	2113.95

where, S_1: Ag NPs; S_2: Curcumin dye and S_3: Ag/Curcumin nanoparticles

4. CONCLUSION

Silver nanoparticles was prepared by pulsed laser ablation and attached with curcumin dye by the volume mixing method with take the ratio the volume mixing of curcumin dye are 0%, 0.25% and 0.50%. XRD and FTIR spectra were used to investigate the structures of targets silver nanoparticles and curcumin dye. The surface morphology of the targets is determined by FE-SEM. the average particle size is 200-220 nm. The impact of elevating the Curc dye concentration on the optical characteristics of AgNPs was examined within the range of 100-1200 nm in wavelength.

The presented work used Z-scan method to examine the non-linear optical properties related to Curc dye, Ag NPs, and Ag/Curc nanocomposites. The samples showed saturable absorption with regard to open aperture Z-scan, while non-linear refractive index for closed aperture Z-scan is shown to be negative (self-defocusing effect). Because of this, samples containing Curc dyes showed less non-linear response, whereas samples containing Ag/Curc NPs showed a large non-linear response. This suggests that the density of the nanoparticles could affect non-linear optical capabilities. Therefore, it was thought that the densities as well as thicknesses of the sample NPs were related to the magnitudes of non-linear optical effects. Through the results obtained. future research using silver nanoparticles and curcumin dye can be used for eradicating cancer tumors, as well as in reducing the activity of bacteria and treatment of water from the biological pollution.

ACKNOWLEDGMENTS

The authors have no funding from any professional official institution. The research was funded at the self-expense of the authors.

REFERENCES

[1] Abdulrahman, H.Z., Ataol, Ç.Y., Jassim, N.M. (2022). Plasmonic enhancement in molecular fluorescence of natural curcumin dye with silver nanoparticles synthesis & biological application. Journal of Pharmaceutical Negative Results, 13(3): 592-603. https://doi.org/10.47750/pnr.2022.13.03.088

[2] Mirzaei, H., Shakeri, A., Rashidi, B., Jalili, A., Banikazemi, Z., Sahebkar, A. (2017). Phytosomal curcumin: A review of pharmacokinetic, experimental and clinical studies. Biomedicine & Pharmacotherapy, 85: 102-112. https://doi.org/10.1016/j.biopha.2016.11.098

[3] Salman, E.A.A., Samawi, K.A., Nassar, M.F., Abdulkareem-Alsultan, G., Abdulmalek, E. (2023). 3D hollow spheres comprising MXene/g-C3N4 heterostructre for efficient polysulfide adsorption and conversion in high-performance Li-S batteries. Journal of Electroanalytical Chemistry, 945: 117629. https://doi.org/10.1016/j.jelechem.2023.117629

[4] Rashid, T.M., Nayef, U.M., Jabir, M.S., Mutlak, F.A.H. (2021). Synthesis and characterization of Au: ZnO (core: shell) nanoparticles via laser ablation. Optik, 244: 167569. https://doi.org/10.1016/j.ijleo.2021.167569

[5] Guidan, Q.A., Mubarak, T.H., Jassim, N.M. (2022). Preparation of aluminum nanoparticles by pulsed laser ablation and its use in reducing iron corrosion. Journal of Optoelectronics Laser, 41(8): 548-557.

[6] El Jery, A., Salman, H.M., Al-Khafaji, R.M., Nassar, M.F., Sillanpää, M. (2023). Thermodynamics Investigation and artificial neural network prediction of energy, exergy, and hydrogen production from a solar thermochemical plant using a polymer membrane electrolyzer. Molecules, 28(6): 2649. https://doi.org/10.3390/molecules28062649

[7] Yao, X., BahrAluloom, Y.J., Jawad, S.F., Abdtawfeeq, T.H., Al-janabi, D.R., Ahmad, N., Alshehri, A.M., Hadrawi, S.K., Al-Taee, M.M., Riadi, Y., Janani, B.J., Fakhri, A. (2023). Multipurpose properties the Z-scheme dimanganese copper oxide/cadmium sulfide nanocomposites for photo-or photoelectro-catalytic, antibacterial applications, and thiamine detection process. Journal of Photochemistry and Photobiology A: Chemistry, 436: 114374. https://doi.org/10.1016/j.jphotochem.2022.114374

[8] Falcão-Filho, E.L., de Araújo, C.B., Rodrigues Jr, J.J. (2007). High-order nonlinearities of aqueous colloids containing silver nanoparticles. Journal of the Optical Society of America B, 24(12): 2948-2956. https://doi.org/10.1364/JOSAB.24.002948

[9] Al-Aaraji, N.A.H., Hashim, A., Hadi, A., Abduljalil, H.M. (2022). Synthesis and enhanced optical characteristics of silicon carbide/copper oxide nanostructures doped transparent polymer for optics and photonics nanodevices. Silicon, 14(15): 10037-10044. https://doi.org/10.1007/s12633-022-01730-7

[10] Van Stryland, E.W., Sheik-Bahae, M. (1997). Z-scan technique for nonlinear materials characterization. In Materials characterization and optical probe techniques: A critical review. SPIE, 10291: 488-511. https://doi.org/10.1117/12.279853

[11] Hussain, M.S., Hassan, Q.M., Sultan, H.A., Al-Asadi, A.S., Chayed, H.T., Emshary, C.A. (2019). Preparation, characterization, and study of the nonlinear optical properties of a new prepared nanoparticles copolymer. Modern Physics Letters B, 33(36): 1950456. https://doi.org/10.1142/S0217984919504566

[12] Jamed, M.J., Alhathal Alanezi, A., Alsalhy, Q.F. (2019). Effects of embedding functionalized multi-walled carbon nanotubes and alumina on the direct contact poly (vinylidene fluoride-co-hexafluoropropylene) membrane distillation performance. Chemical Engineering Communications, 206(8): 1035-1057. https://doi.org/10.1080/00986445.2018.1542302

[13] Samawi, K.A., Salman, E.A.A., Alshekhly, B.A.A., Nassar, M.F., Borzehandani, M.Y., Abdulkareem-Alsultan, G., Alif Mohammad Latif, M., Abdulmalek, E. (2022). Rational design of different π-bridges and their theoretical impact on indolo [3, 2, 1-jk] carbazole based dye-sensitized solar cells. Computational and Theoretical Chemistry, 1212: 113725. https://doi.org/10.1016/j.comptc.2022.113725

[14] Alwan, S.H., Salem, K.H., Alshamsi, H.A. (2022). Visible light-driven photocatalytic degradation of Rhodamine B dye onto TiO_2/rGO nanocomposites. Materials Today Communications, 33: 104558. https://doi.org/10.1016/j.mtcomm.2022.104558

[15] Gamernyk, R., Periv, M., Malynych, S. (2014). Nonlinear-optical refraction of silver nanoparticle composites. Optica Applicata, 44(3): 389-398. http://dx.doi.org/10.5277%2Foa140304

[16] Mustafa, M.A., Abdullah, A.R., Hasan, W.K., Habeeb, L.J., Nassar, M.F. (2021). Two-way fluid-structure interaction study of twisted tape insert in a circular tube having integral fins with nanofluid. Eastern-European Journal of Enterprise Technologies, 3(8): 111. https://doi.org/10.15587/1729-4061.2021.234125

[17] Thomas, J., Perikaruppan, P., Thomas, V., John, J., Mathew, R.M., Thomas, J., Rejeena, I., Mathew, S., Mujeeb, A. (2018) Morphology dependent nonlinear optical and photocatalytic activity of anisotropic plasmonic silver. RSC Advances, 72(8): 41288-41298.

[18] Parsaee, F., Fayzullaev, N., Nassar, M.F., Abd Alreda, B., Mahmoud, H.M., Taki, A.G., Faraji, M. (2024). Co-Fe dual-atom isolated in N-doped graphydine as an efficient sulfur conversion catalyst in Li-S batteries. Journal of Alloys and Compounds, 988: 174136. https://doi.org/10.1016/j.jallcom.2024.174136

[19] John, J., Thomas, V., Baby, S., Mathew, S., Rejeena, I., MUJEEB, A. (2022). Open-aperture Z-scan and optical limiting of plasmonic silver-polymer system. Journal of Optoelectronics and Advanced Materials, 24(5-6): 250-255.

[20] Samawi, K.A., Abdulrazzaq, S.J., Zorah, M., Al-Bahrani, M., Mahmoud, H.M., Abdulkareem-Alsultan, G., Taki, A.G., Nassar, M.F. (2024). MoS_2/graphdiyne nanotube/MXene 3D-interconnected ternary aerogel: A high-performance electrocatalyst for hydrogen evolution reaction. Journal of Solid State Chemistry, 334: 124690. https://doi.org/10.1016/j.jssc.2024.124690

[21] Hossain, M.K., Toki, G.I., Samajdar, D.P., Mushtaq, M., Rubel, M.H.K., Pandey, R., Madan, J., Mohammed, M.K.A., Islam, M.R., Rahman, M.F., Bencherif, H. (2023). Deep insights into the coupled optoelectronic and photovoltaic analysis of lead-free $CsSnI_3$ perovskite-based solar cell using DFT calculations and SCAPS-1D simulations. ACS Omega, 8(25): 22466-22485. https://doi.org/10.1021/acsomega.3c00306

[22] Mohammed, M.K., Jabir, M.S., Abdulzahraa, H.G., Mohammed, S.H., Al-Azzawi, W.K., Ahmed, D.S., Singh, S., Kumar, A., Asaithambi. S., Shekargoftar, M. (2022). Introduction of cadmium chloride additive to improve the performance and stability of perovskite solar cells. RSC Advances, 12(32): 20461-20470. https://doi.org/10.1039/D2RA03776A

[23] Naderali, R., Golzan, M. (2022). Nonlinear optical properties of silver nanoparticles produced by laser ablation. International Journal of Optics and Photonics, 16(2): 187-200. http://doi.org/10.52547/ijop.16.2.187

[24] Samawi, K.A., Salman, E.A.A., Hasan, H.A., Mahmoud, H.M., Mohealdeen, S.M., Abdulkareem-Alsultan, G., Abdulmalek, E., Nassar, M.F. (2024). Single-atom cobalt encapsulated in carbon nanotubes as an effective catalyst for enhancing sulfur conversion in lithium-sulfur batteries. Molecular Systems Design & Engineering, 9(5): 464-476. https://doi.org/10.1039/D3ME00191A

[25] Badran, H.A., Ajeel, K.I., Lazim, H.G. (2016). Effect of nano particle sizes on the third-order optical non-linearities and nanostructure of copolymer P3HT: PCBM thin film for organic photovoltaics. Materials Research Bulletin, 76: 422-430. https://doi.org/10.1016/j.materresbull.2016.01.005

[26] Henari, F.Z., Patil, P.S. (2014). Nonlinear optical properties and optical limiting measurements of {(1Z)-[4-(Dimethylamino) Phenyl] Methylene} 4-Nitrobenzocarboxy Hydrazone Monohydrate under cw laser regime. Optics and Photonics Journal, 4(7). https://doi.org/10.4236/opj.2014.47018

[27] González-Castillo, J.R., Rodriguez-Gonzalez, E., Jiménez-Villar, E., Cesar, C.L., Andrade-Arvizu, J.A. (2017). Assisted laser ablation: silver/gold nanostructures coated with silica. Applied Nanoscience, 7(8): 597-605. https://doi.org/10.1007/s13204-017-0599-2

[28] Shanshool, H.M., Yahaya, M., Wan, M.M.Y., Abdullah, Y.I. (2016). Third order nonlinearity of PMMA/ZnO nanocomposites as foils. Optical & Quantum Electronics, 48(1):1-14. https://doi.org/10.1007/s11082-015-0267-2

[29] Samawi, K.A., Mohammed, B.A., Salman, E.A.A., Mahmoud, H.M., Sameen, A.Z., Mohealdeen, S.M., Abdulkareem-Alsultan, G., Nassar, M.F. (2024). Vertical growth of a 3D Ni-Co-LDH/N-doped graphene aerogel: A cost-effective and high-performance sulfur

host for Li-S batteries. Physical Chemistry Chemical Physics, 26(12): 9284-9294. https://doi.org/10.1039/D3CP05716J
[30] Khan, I., Saeed, K., Khan, I. (2019). Nanoparticles: Properties, applications and toxicities. Arabian Journal of Chemistry, 12(7): 908-931. https://doi.org/10.1016/j.arabjc.2017.05.011
[31] Gondal, M.A., Drmosh, Q.A., Yamani, Z.H., Saleh, T.A. (2009). Synthesis of ZnO_2 nanoparticles by laser ablation in liquid and their annealing transformation into ZnO nanoparticles. Applied Surface Science, 256(1): 298-304. https://doi.org/10.1016/j.apsusc.2009.08.019